

UDC 539.3

FEATURES OF FINITE ELEMENT MODELING FOR BUCKLING ANALYSIS OF ELASTIC SHELLS WITH INHOMOGENEOUS STRUCTURE UNDER THERMOMECHANICAL LOADS

O.P. Krivenko¹,

Candidate of Science (Engineering), Senior Researcher

P.P. Lizunov¹,

Doctor of Science (Engineering), Professor

O.B. Kalashnikov²,

Candidate of Science (Engineering)

¹*Kyiv National University of Construction and Architecture, Kyiv*

²*State Scientific and Technical Center for Nuclear and Radiation Safety, Kyiv*

DOI: 10.32347/2410-2547.2026.116.50-66

Some practical issues of computer modeling and analysis of geometrically nonlinear deformation processes of thin shells with stepwise variable thickness under static thermomechanical loading are considered. The methodology for studying shell systems with various structural elements in the thickness direction is based on the use of a modifiable universal three-dimensional finite element with additional variable parameters.

Keywords: thin inhomogeneous shell, geometrically nonlinear deformation, buckling, thermomechanical loading, universal three-dimensional finite element, moment finite-element scheme

Introduction

Methods and algorithms for the analysis of flexible plates and shells continue to attract considerable attention from researchers. First of all, this concerns methods for analyzing the stress-strain state and buckling of such structures. The process of shell buckling and its subsequent deformation often determines the ultimate load-bearing capacity of a structure. These issues are particularly important when analyzing flexible elastic shells with variable thickness subjected to thermomechanical loading.

Most results related to the geometrically nonlinear deformation and buckling analysis of shells have been obtained using numerical methods. Among them, the finite element method [1-9] occupies a leading position and is most often applied in the form of the displacement method. In recent years, the semi-analytical finite element method has gained wide recognition and demonstrated high efficiency [10-12]. Studies devoted to the buckling analysis of elastic shells of inhomogeneous composition based on the finite element method are presented in [13-17].

In general, thin-walled shell structures, depending on their functional purpose, may combine various structural inhomogeneities such as ribs and cover plates, reinforced and non-reinforced holes, cavities, channels, local thickening and thinning, sharp bends in the mid-surface, and other features, multilayer material structures, as well as complex mid-surface geometries that cannot be described by simple analytical expressions. During operation, shell structures are often subjected to static mechanical and thermal fields, resulting in nonlinear deformation behavior. Methods for analyzing the behavior of such shells remain insufficiently developed due to the complexity of accounting for all the above-mentioned factors in the formulation of the governing equations. Therefore, the use of universal computational models and technologies for studying shells with complicated geometric structures is promising and contributes to the further development of the finite element method.

The study of nonlinear deformation, buckling and natural vibrations of inhomogeneous shell structures of complex shape under thermomechanical loading using the application of finite element modeling techniques is presented in [14-17]. There are the theoretical foundations of the developed method and a large number of benchmark and new problems demonstrating its efficiency. The present paper continues the series of works by the authors cited in [14-17] and other related publications. It is devoted to the specific features of the practical application of the algorithm for buckling and natural

vibrations analysis of structurally inhomogeneous shells under complex combined thermomechanical loading.

1. Problem statement and research method

A method for solving static buckling problems of thin elastic shells of inhomogeneous structure under external mechanical loads and non-uniform volumetric heating is considered. The inhomogeneity of a shell, interpreted in a broad sense, includes the following aspects: a complex geometric structure of the shell (i.e., a complex shape of the mid-surface and various irregularities (geometric features) in the thickness direction (Fig. 1)); structural inhomogeneity of the shell material the form of combinations of different multilayer packages; different boundary conditions applied to individual shell areas; and non-uniform thermomechanical loading [14, 15].

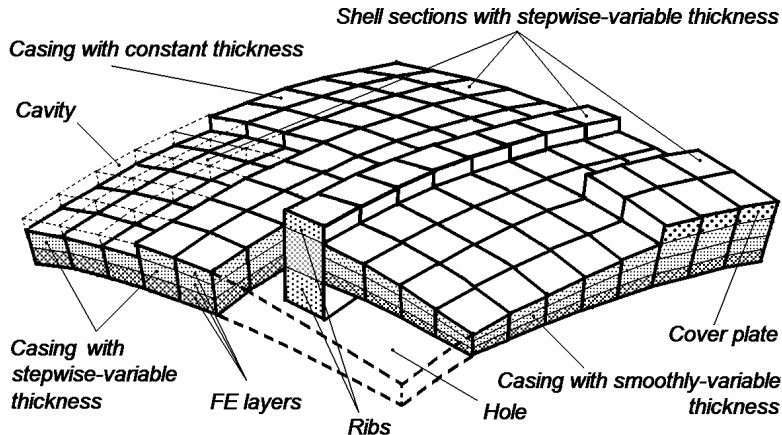


Fig. 1. Fragment of the finite element model of a shell with inhomogeneous structure

Each type of geometric feature of shell elements is associated with specific characteristics of the stress–strain state, buckling processes, and natural vibrations of the structure. This requires an appropriate representation in the governing equations of the corresponding shell theory. Conventionally, various finite elements are used for the analysis of such shells, constructed either on the basis of shell theories or on the three-dimensional theory of elasticity. The simultaneous consideration of different geometric features requires the development of computational methods for shells of a generalized class. One such approach is based on the use of universal finite elements [14–17].

The finite element methodology [14–17] for analyzing the stress–strain state, buckling, and post-buckling behavior of inhomogeneous shells is based on the geometrically nonlinear relationships of the three-dimensional theory of thermoelasticity [18–20], the principles of the moment finite-element scheme (MFES) [5, 13], and the use of a modifiable universal three-dimensional finite element with additional variable parameters. This unified approach made it possible to construct a single computational finite element model of a shell with inhomogeneous structure.

Geometrically, the shell is treated as a three-dimensional body possessing certain specific features. The body's dimension in the thickness direction is much smaller than its in-plane dimensions (i.e., the shell is thin), and the compressive stress through the thickness of the shell layer (single-layer or multilayer) is assumed to be constant. Shell sections are considered as areas of continuously varying thickness (with a smooth mid-surface and with sharp bends in the mid-surface) and stepwise thickness (sections containing the casing, ribs, cover plates, cavities, channels, holes, etc.). The term “casing” refers to the shell body without geometric irregularities through the thickness. The non-classical kinematic hypothesis of the deformed straight line is used in governing equations [14]. The universal three-dimensional finite element with additional variable parameters is developed on the basis of an isoparametric three-dimensional finite element with polylinear shape functions for coordinates and displacements. A distinctive feature of the finite element is its modification for modeling all sections of the shell with stepwise thickness. The initial assumptions, fundamental theoretical provisions, and governing relations underlying the finite element procedure for the investigation of buckling and

natural vibrations of thin elastic inhomogeneous shells under complex combined thermomechanical loading are presented in [14–17]. Below, the corresponding algorithm constructed on these approaches is briefly outlined; we refer to it as the MFES method.

2. Algorithm for buckling and natural vibration analysis of shells

The study of geometrically nonlinear deformation processes of shells is based on the Lagrangian formulation of the incremental variational problem. The deformation process of the structure is

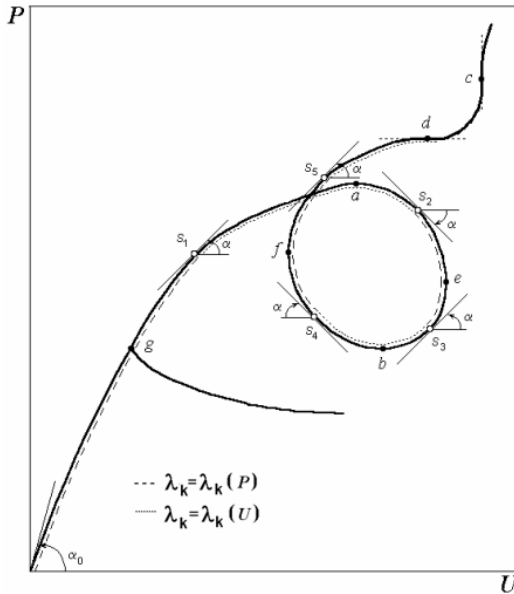


Fig. 2. General appearance of the $P-U$ curve, selection of the continuation parameter λ_k and limits of its variation

represented as a sequence of equilibrium states corresponding to sufficiently small increments of thermomechanical loading. The new geometry and the deformation history of the shell are assumed to be known at the current load step. An integral approach is employed to analyze the shell behavior under static thermomechanical loading. The algorithm is constructed as follows (Fig. 2).

The static problem of geometrically nonlinear deformation and buckling of an elastic shell is solved by a step-by-step method. Within this approach, each load step corresponds to an increment (positive or negative) of the external load parameter P . The parameter P is a generalized parameter of thermomechanical loading $P = (Q, T)$ that defines the combined effect of various static mechanical Q and thermal T fields acting on the shell.

The solution of the static nonlinear stability problem is represented by the relationship between the external load parameter P and the displacement field of a characteristic point of the finite-element shell model (FESM). This relationship is determined at each increment of the generalized load parameter P and is characterized by the «load P – deflection U » ($P-U$) curves for selected points of the shell (Fig. 2). The algorithm is based on the generalized $P-U$ curve in the form of a loop with a branching point g and special points $a-f$. At each increment of the generalized load parameter ΔP , the stress-strain state of the shell is determined too. The updated shell coordinates (its deformed configuration) and the increments of displacement and stress fields are computed. These results serve as the initial data for the modal analysis of the prestressed and deformed structure, as well as for the subsequent calculation step.

The algorithm for solving the stability problem of the shell employs the parameter continuation method, an iterative procedure based on the modified Newton–Kantorovich method, and a technique for adjusting the algorithm parameters [14, 15]. A specific feature of the developed algorithm for solving the nonlinear stability problem is the automated control of the continuation parameter type during the solution process. This makes it possible to obtain the entire $P-U$ regardless of its shape and complexity.

At a given step, the continuation parameter λ_k may be either the parameter of the external nodal thermomechanical loading $P = P(Q, T)$ or the controlling displacement U of the FESM, selected by the algorithm. The controlling displacement u_v^i corresponds to the displacement of the node “ v ” of the FESM at which the increment of the magnitude of the nodal displacement vector has been the largest in the previous step. The necessity to change the continuation parameter arises in the neighborhood of special points of the $P-U$ curves, as illustrated in Fig. 2. The portions of the $P-U$ curve where the load parameter $\lambda_k = \lambda_k(P)$ is used as the continuation parameter are shown by a

dashed line $(0 - s_1, s_2 - s_3, s_4 - s_5)$, whereas the portions where the continuation parameter is the displacement of the controlling node, i.e., $\lambda_k = \lambda_k(U)$, are indicated by dotted lines $(s_1 - s_2, s_3 - s_4, s_5 - \dots)$.

The selection of the continuation parameter type for each subsequent load step $k+1$ is performed depending on the fulfillment, at the previous step, of condition:

$$\left| \Delta P_k / \Delta u_k^{i'} \right| \geq C \left| \Delta P_1 / \Delta u_1^{i'} \right|, \quad (1)$$

where ΔP_1 , ΔP_k and $\Delta u_1^{i'}$, $\Delta u_k^{i'}$ – are the load increments and increments of nodal displacements at the first and at the k -th steps, respectively; $C = 0.1$ – is a correction coefficient that allows adjustment of the location of the points where the continuation parameter is switched on the $P-U$ curve.

It should be noted that the load parameter $\lambda(P)$ is taken as the continuation parameter at the first step ($P = P(Q, T) = P(0, 0) = 0$).

An important issue is the proper selection of the magnitude of the first load step ΔP_1 . In the case of purely mechanical loading, the magnitude of the first step $\Delta P_1 = \Delta Q_1$ may be chosen relatively arbitrarily. As a rule, it is prescribed within sufficiently wide limits ($1/100 \div 1/3$) typically a certain percentage of the specified final load Q_{max} . During further calculations, the load step size is automatically adjusted by the algorithm. Experience in solving problems of nonlinear deformation and stability of heterogeneous shells has shown that the initial step size has practically no influence on the total computation time. Specially developed procedures rapidly establish rational values for the subsequent load increments.

However, in the case of thermal loading, the magnitude of the first increment $\Delta P_1 = \Delta T_1$ must be small. This is due to the volumetric effect of the temperature field on the shell. The magnitude of the first temperature load increment should not exceed 1°C . The subsequent increments of the temperature loading may then be gradually increased automatically by a factor of approximately 1.3. It should be noted that solving problems involving purely thermal loading requires a reduction of the accuracy parameter ε by 6–8 orders of magnitude compared to the case of mechanical loading, namely to about $\varepsilon = 10^{-8} \div 10^{-12}$ instead of $\varepsilon = 10^{-2} \div 10^{-4}$.

Under combined thermomechanical loading, the magnitude of the first load increment $\Delta P_1 = \Delta P_1(\Delta Q_1, \Delta T_1)$ should be chosen within the range ($1/100 \div 1/10$).

According to the geometric interpretation of the components in condition (1), this condition can be expressed in the following form:

$$\tan \alpha \geq C \tan \alpha_0, \quad (2)$$

where α_0 is the angle of inclination of the tangent to the $P-U$ curve computed at the first load step (Fig. 1), and α is the corresponding angle of inclination of the tangent to the curve $P-U$ curve at the k -th step.

If condition (2) is satisfied, the continuation parameter is taken to be the parameter of the external nodal load field, $\lambda_k(P)$. Otherwise, the continuation parameter is chosen as the component of the controlling generalized nodal displacement vector $u_v^{i'}$ of the FESM that has the maximum absolute value, i.e., the displacement parameter $\lambda_k(U)$.

After completing at the k -th step the main procedure of the general algorithm (namely, the iterative modified Newton–Kantorovich method) the problem is considered solved for that step. The computed results are then collected into files for further post-processing, performing modal analysis of the prestressed structure, and continuing the solution at the next $k+1$ step.

For performing the modal analysis of the shell, files containing the necessary information are generated. At this stage of the integrated calculation, a modal analysis is carried out with the updated

deformed configuration of the shell $\{x_k^{i'}\} = \{x_{k-1}^{i'}\} + \{u_k^{i'}\}$ and its prestressed state $\{\sigma_k^{ij}\} = \{\sigma_{k-1}^{ij}\} + \{\Delta\sigma_k^{ij}\}$ resulting from the applied thermomechanical load ΔP_k . The stress-strain state obtained at step k is taken as the initial equilibrium configuration relative to which the small vibrations of the shell are analyzed. The natural frequencies ω_i^k (ω_1^k as shown in Fig. 3) and the corresponding vibration modes of the shell are determined. The required number of vibration frequencies is usually specified in advance as input data. Thus, in the finite element formulation used for the modal analysis, both the deformed configuration of the structure and the stresses accumulated in the previous $k-1$ steps are taken into account $\sigma_{k-1}^{ij} = \sum_{r=1}^{k-1} \Delta_r \sigma^{ij}$.

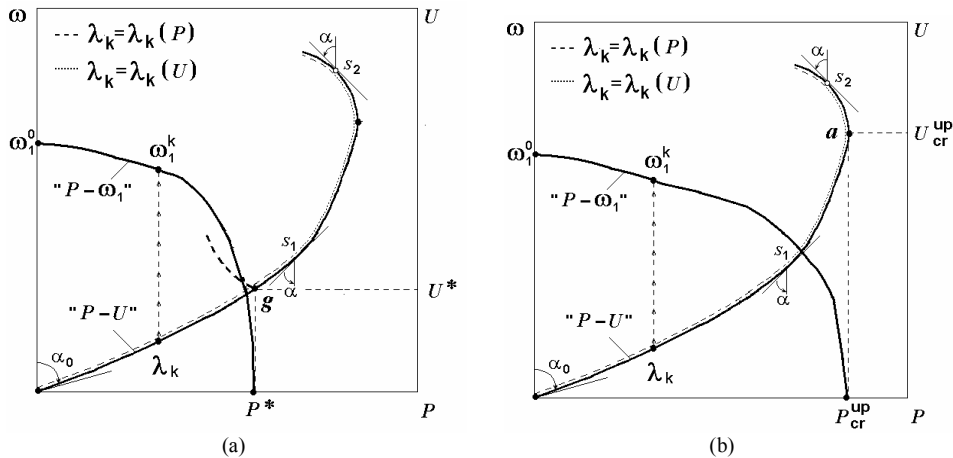


Fig. 3. Integrated algorithm of problems of nonlinear deformation, stability, and natural vibrations of flexible shells

The result of the modal analysis is presented as a «load P – lowest frequency ω_1 » ($P - \omega_1$) curve (Fig. 3). If there is a branching point g on the $P-U$ curve in the pre-buckling domain of the shell (Fig. 3a) corresponding to the load value P^* , then at this point the lowest natural frequency of the shell becomes zero ($\omega_1 = 0$). This load P^* can be taken as the upper critical load according to the dynamic criterion. If no branching point exists in the pre-buckling domain (Fig. 3b), the point a corresponding to the maximum of the $P-U$ curve represents the upper critical load P_{cr}^{up} , both according to the static and the dynamic criteria ($\omega_1 = 0$).

Thus, a distinctive feature of the method and the algorithm developed on its basis is the ability to accurately analyze both the pre-buckling and post-buckling states of shell deformation, including shells with various thickness features such as ribs, channels, and similar structural elements. Furthermore, the developed algorithm allows for the detection of possible solution branching points on the $P-U$ curve, both in the pre-buckling domain and in other areas of the curve.

3. Special points on the load–deflection curves

A unique characteristic of the developed algorithm, which implements the methodology [13–17], is its ability to identify and analyze special points on the $P-U$ curve during the calculation of shell buckling. This approach allows the solution to be traced in the neighbourhood of these points and enables traversal of the entire curve regardless of its complexity.

In general, the $P-U$ curve can have an arbitrary shape (Fig. 2). In the figure, the $P-U$ curve is shown as a loop containing a number of special points, including the branching point g . Points a

and b on the curve are referred to [21] as the upper P_{cr}^{up} and lower P_{cr}^{lw} critical points, respectively. Points e and f are turning points, and the curve may also include inflection points c and d .

Typically, the special points on the $P-U$ curve correspond to real physical phenomena and quantities. Their presence introduces certain mathematical challenges and imposes specific requirements on the algorithm for solving the nonlinear stability problem. Implementing the ability to switch continuation parameters (from load $\lambda(P)$ to displacement $\lambda(U)$ and vice versa) at any stage is extremely important for ensuring reliable nonlinear analysis of shell stability.

At the critical points a and b , the generalized derivative $\partial P/\partial U = 0$ is zero. The point a corresponds to an unstable deformation mode of the shell. Buckling occurs through a sudden change in the shell's shape – often referred to as snap-through buckling. In static shell stability problems, the upper critical load P_{cr}^{up} is taken as the load corresponding to the first upper critical point. The point b corresponds to the lower critical load P_{cr}^{lw} , below which buckling of the shell cannot occur. In the stepwise continuation algorithm, the solution passes through these points when in their neighbourhood the continuation parameter is taken as the controlling displacement U .

At the turning points e and f , where the generalized derivative $\partial P/\partial U = \infty$, the sign of the displacement increment U changes. In the neighbourhood of these points, the continuation parameter is the load parameter P .

The inflection points c and d are characterized by second derivatives $\partial^2 P/\partial U^2 = \infty$ and $\partial P/\partial U = 0$, respectively. In the nonlinear algorithm, these points fall under one of the special point types described above. Therefore, to traverse the curve through point c ($\partial P/\partial U = \infty$), the continuation parameter is taken as the load parameter P , whereas in the neighbourhood of the point d ($\partial P/\partial U = 0$), the continuation parameter is the controlling displacement U .

4. Method for determining the solution branching point

The appearance of a branching point g on the $P-U$ curve (Fig. 2) is associated with the emergence of adjacent equilibrium forms during shell deformation. The behavior of the shell in the vicinity of branching points g is characterized by a smooth variation of the stress–strain state. This process corresponds to a loss of stability in the infinitesimal sense. The load value P^* corresponding to the first branching point is sometimes taken as the upper critical load. The algorithm uses three approaches to identifying branching points g .

4.1. First method (i). From a mathematical standpoint, the linearized matrix of the governing equations degenerates in the neighbourhood of a branching point g . Therefore, the algorithm performs an analysis of the linearized matrix for singularity at each load step to determine the location of the branching points [5].

Thus, to identify a branching point the qualitative theory is used, which involves analyzing the eigenvalues of the linearized stiffness matrix [5, 14, 22]. The presence of the branching point within the integration interval is associated with a mandatory sign change of those eigenvalues that are zero at this point. Accordingly, the number of eigenvalues that change sign at the current continuation step is determined. This procedure is implemented using the Gauss elimination process, which reduces the matrix to triangular form. The number of positive and negative diagonal entries corresponds to the number of positive and negative eigenvalues. The appearance of at least one negative eigenvalue of the linearized stiffness matrix indicates an unstable deformation mode of the shell [5]. Since the shell stability problem is solved step-by-step, the branching points in this approach are registered by the algorithm with an accuracy corresponding to the load increment at the current step.

4.2. Second method (ii). To more accurately determine the presence of a possible branching point and draw adjacent deformation modes in its vicinity, the following methodology is used. The adjacent deformation mode is identified by introducing a perturbation defined by the parameter η into the perfect initial shell configuration. If η is small, its influence is observed near the branching point on

the $P-U$ curve. Most commonly, this perturbation takes the form of a small initial geometric imperfection of the shell's mid-surface, deviating from its perfect shape. Studies have shown that an effective approach is to introduce a imperfection corresponding to the shell's lowest natural vibration mode as the system approaches the branching point g . In the pre-buckling domain, this imperfection can transform the branching point into a critical point P^* . Other possible perturbations may involve deviations introduced into the boundary conditions, load parameters, or similar aspects of the system.

4.3. Third method (iii). In addition, the developed integrated algorithm (Fig. 3) for the combined solution of shell stability and modal analysis problems under thermomechanical loading also allows for the identification of the first branching point in the pre-buckling domain, if it exists. This approach corresponds to the dynamic stability criterion.

The use of these three methods for detecting a branching point g in the pre-buckling domain is important from the standpoint of preventing potential failure scenarios during the design stage of shell structures, thereby mitigating the risk of accidents that could occur during their operation.

5. Methodology for modeling complex combined thermomechanical loads on a inhomogeneous shell

During operation, shell structures are often subjected to various mechanical and thermal fields. A distinctive feature of the algorithm is the methodology used to define the thermomechanical load as a function. This approach allows for a realistic description of the thermomechanical effects on the structure. Given the potential for extreme operating conditions, these effects can be quite complex.

The principles of the loading methodology used are as follows.

5.1. If the *type* of thermomechanical loading remains *unchanged*, i.e., it does not depend on the load step, the load at all stages is described by the same function. This function reflects the load distribution only in the shell's plan. In this case, it is recommended to establish a correspondence between the load parameter and either the element numbers of the FESM or the mesh coordinates in the plan, $I2 = \overline{1, M2}$ and $I3 = \overline{1, M3}$.

5.1.1. For types of mechanical loading such as uniformly distributed pressure over the entire shell plan or part of it, concentrated forces, and similar cases, the application of the load poses no particular difficulties and is practically standard. Similarly, describing planar thermal loading (whether uniform or non-uniform through the shell thickness) is also straightforward. In the case of thickness-wise non-uniform heating, it is only necessary to distinguish between the top and bottom nodes of the FESM to correctly represent the applied temperature field.

A more *complex* case arises when the thermomechanical loading *varies within the shell plan*.

5.1.2. The first example is the non-uniform planar heating of an axisymmetric shell [14, 23]. The temperature field through the shell thickness is assumed to be constant. The panel heating is considered for two cases of the radial temperature distribution along the radius $\bar{r} = r/a$, where a is the radius of the support contour (Fig. 4):

$$T(t, \bar{r}) = t(1 - \bar{r}^2), \tag{3}$$

$$T(t, \bar{r}) = t\bar{r}^2. \tag{4}$$

The temperature parameter $t = \text{const}$ is prescribed. That is, the function $T(t, \bar{r})$ varies only along the panel radius and depends on the given parameter t .

By associating the FESM mesh coordinate $I2$ with the radius of the shell's support contour, the loading function

can be easily obtained. Indeed:

$$\bar{r}_{I2} = \frac{\bar{r}}{M2-1} \cdot (I2-1), \quad I2 = \overline{1, M2}.$$

Then, for the functions (3) and (4), we have:

$$T(t, \bar{r}_{I2}) = t(1 - \bar{r}_{I2}^2); \quad T(t, \bar{r}_{I2}) = t\bar{r}_{I2}^2. \tag{5}$$

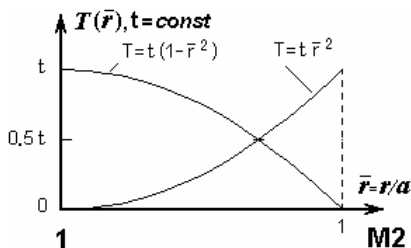


Fig. 4. Temperature field distribution along the panel radius

5.1.3. A more complex case is the non-uniform heating of shells with stepwise-varying thickness, such as shells with ribs (Fig. 5a) or with channels (Fig. 5b)

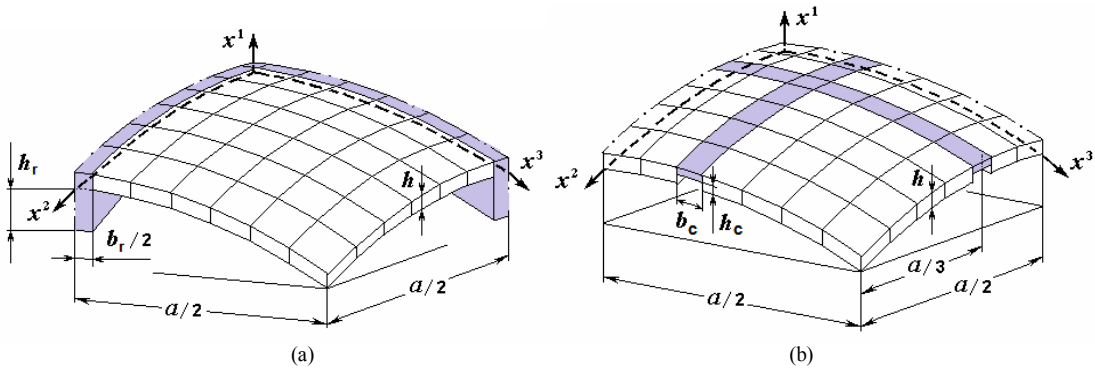


Fig. 5. Fragments of the FESM with ribs (a) and channels (b)

The following shell element heating options are considered: a shell's casing (without geometric features along its thickness) is heated by T^{sc} degrees, while areas with ribs or channels are heated by T^r or T^o degrees, respectively. Examples of heating of shell elements:

(I) uniform heating/cooling of the entire panel;

(II) uniform heating/cooling of the casing by T^{sc} degrees, while the sections with ribs or channels remain, for example, unheated $T^r=0/T^c=0$;

(III) uniform heating/cooling of the sections with ribs or channels by T^r / T^c degrees, while the casing remains unheated $T^{sc}=0$.

The first heating case, uniform heating/cooling of the entire panel, is implemented in the standard way for the finite element method.

The second and third cases, when the casing and the sections with ribs / channels are subjected to different temperatures, require the use of a special procedure.

In the case of ribs, narrow elements are used at the boundary between the casing and the ribbed sections. The casing temperature T^{sc} is set at those nodes of these finite elements that border other casing finite elements (named as CFEs). The intermediate elements are also the CFEs. The rib element temperature is set at other nodes of the narrow finite elements that border the ribbed elements. This procedure is shown schematically in Figure 6.

According to accepted terminology [14–17], a universal finite element modeling sections with ribs or channels is called a modifiable finite element (MFE). In ribbed sections, it is designated as the MFE^+ , and in sections with channels, as the MFE^- .

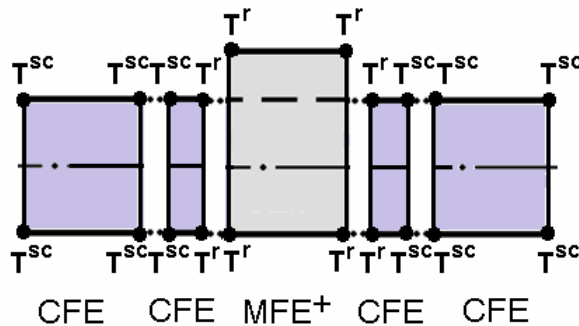


Fig. 6. Heating/cooling of the casing by T^{sc} degrees and the shell section with a rib by T^r degrees

In the case of a section with channels (Fig. 7), the narrow finite element (MFE⁻) is located on the channel side. The casing temperature T^{sc} is set at those nodes of the intermediate element that border the CFE. The channel element temperature T^c is set at other nodes of the narrow finite element.

This approach allows for the assignment of nodal temperatures according to different heating laws for shells with stepwise-varying thickness.

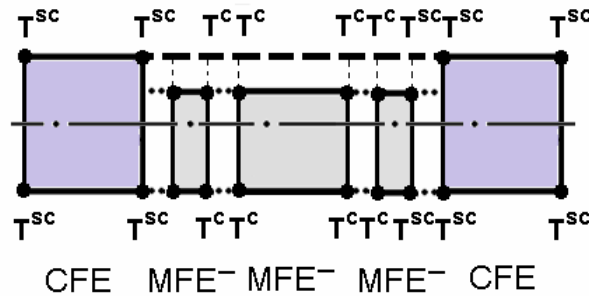


Fig. 7. Heating/cooling of the casing by T^{sc} degrees and the shell section with a channel by T^c degrees

Such loadings occur, for example, in the analysis of spacecraft (with ribs and channels) during atmospheric entry or re-entry. Significant stresses can develop in the shell panel due to the differing rates of heating between the panel itself and its structural elements, namely ribs and channels [14, 15, 24–26]. For instance, in the presence of channels and cavities in the structure, the thinned sections heat up faster than the shell panel at the initial stage of atmospheric entry, while the panel remains relatively cool. The cold panel restricts the thermal expansion of the heated sections, which can lead to their compression and potential global instability of the shell. Later, the channel sections may cool faster than the panel, with the cooler channel areas limiting the overall expansion of the shell. This can cause local buckling of the panel due to the compressive stresses generated. Similarly, when ribs reinforce the shell, complex thermomechanical loading produces comparable deformation and stability loss processes.

5.2. If the *type* of thermomechanical loading *changes* during the loading process, different modes of thermal and mechanical influence are considered sequentially. The moment of transition between loading modes depends on the specified value of the load parameter $P_k = P_n^0$, where P_n^0 is the predetermined load at which the loading mode changes, and $n \geq 2$ is the total number of loading modes.

For each loading mode n , a corresponding function $P^n = P^n(Q, T)$ is prescribed, which describes the distribution of thermomechanical loading across the shell plan. When changing the loading mode for each new combined loading scenario, it is necessary to redefine the algorithm control parameters to account for the new loading law. *This is important!*

This approach allows not only the specification of different thermomechanical loading laws across the shell plan, but also the handling of various transitions between loading modes.

5.2.1. For example, consider preheating a shell followed by loading it with uniform pressure while keeping the temperature field fixed. This situation involves two distinct thermomechanical loading modes. In the first stage of the analysis (loading mode $n = 1$), the algorithm parameters must be set as for thermal loading. In the second stage (loading mode $n = 2$), the parameters must be redefined as for combined thermomechanical loading.

5.2.2. Another example of a complex thermomechanical loading regime on a shell is as follows. The shell is subjected simultaneously to uniform heating and pressure. When the pressure intensity q reaches a certain value q^0 , the panel heating stops at a temperature $T = T_0^\circ\text{C}$. From this moment onward, the pressure continues to change while the temperature field remains fixed. Again, two thermomechanical loading modes are present.

To implement the first mode of simultaneous thermomechanical influence ($n = 1$), a relationship between mechanical and thermal loading must be established. For instance, this could be a law in which,

for each 1° increase in temperature, the pressure increases by a specified amount. The next mode ($n = 2$) corresponds to the further variation of pressure under a fixed (unchanging) temperature field.

The use of the developed methodology of specifying thermomechanical loading as a function allows modeling of combined and complex operational loads on shell structures that closely resemble real conditions. This, in turn, enables a more accurate assessment of the effect of loading regimes on the system’s stability, allows a more detailed study of the structural elements’ behavior, and helps predict the shell’s response under various operational scenarios.

6. Numerical calculations and analysis of results

A series of specially selected problems illustrate and explain certain features of the developed method. The setups and solutions of stability problems for inhomogeneous shells under action of thermomechanical loads are considered.

6.1. The capabilities of the method for determining solution branching points g are illustrated using the classical problem [27-29] of determining the critical load for a shallow, axisymmetric, spherical panel rigidly clamped along its contour. The shell is subjected to a uniform pressure of intensity q . The possibility of the appearance of axisymmetric (AM) and non-axisymmetric (NAM) modes of instability for panels with different curvatures $k = H/h$ is investigated. The curvature variation is achieved by changing the panel thickness h while keeping the rise $H = 5$ constant. Three approaches for determining the branching points g using the developed method (see Section 4) are considered.

The dependence of the dimensionless critical load \bar{q}_{cr}^e on the dimensionless shallowness parameter

$b = \sqrt{6.6k}$ of the axisymmetric spherical panel demonstrates the effectiveness of the applied approaches (Fig. 8):

$$\bar{q}_{kp}^e = \frac{q_{kp}^e}{E} \frac{\sqrt{12(1-\nu^2)}}{4} \left(\frac{R}{h}\right)^2,$$

where R – is the radius of the spherical shell, E – is the Young’s modulus, ν – is the Poisson ratio.

The branching points are determined using three approaches:

- (i) by counting the number of negative eigenvalues (denoted in Fig. 8 as MFES, $\eta = 0$);
- (ii) by introducing a small perturbation into the initial shape of the shell (MFES, $\eta = 0.001$);
- (iii) by modal analysis (MFES, MA).

The obtained solutions show good agreement with the corresponding results reported by other authors. A detailed analysis of the results can be found in [17].

The main principles of the methodology for specifying complex thermomechanical loading are illustrated using three representative problems. These examples of defining the load as a function allowed obtaining solutions to practically important tasks and demonstrated the effectiveness of the developed approach in the study of shell buckling.

6.2. The influence of a thermomechanical load, consisting of two action regimes, on the stability of a thin shell of constant thickness h is considered. The axisymmetric shell is hinged along its contour ($\bar{u} = 0$). The input data are: $H = 4h$, $h = 1$ cm, $a = 100h$, $\alpha = 0.125 \cdot 10^{-4}$ grad $^{-1}$ is a coefficient of linear thermal expansion. The calculation results are presented in the figures using the dimensionless parameters $\bar{q} = a^4 q / (Eh^4)$ and $\bar{u}' = u' / h$.

The influence on the shell’s stability of a uniform volumetric preheating to a specified temperature T ($T = 0, +20, +40^\circ\text{C}$) and subsequent loading by an external uniform pressure of intensity q is studied.

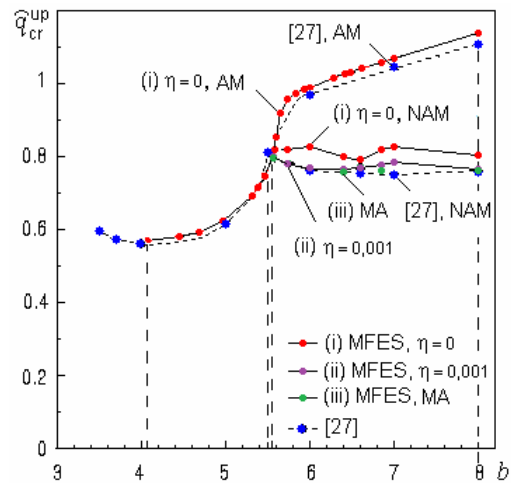


Fig. 8. Dependence of the critical load on curvature for axisymmetric spherical shells

In other words, the panel is subjected to two regimes of thermomechanical loading, which in the algorithm are implemented as a combined sequential loading process. This process is carried out in two stages, meaning that the *type* of thermomechanical action *changes* during loading (see 5.2.1). At each stage of the thermomechanical loading, however, the *type* of influence remains *constant* (see 5.1.1).

At the first stage ($n=1$), the panel undergoes a uniform volumetric heating, which induces nonlinear deformation of the shell and serves as a preliminary perturbation of its stress–strain state. At the second stage ($n=2$), the pressure acts under the fixed temperature field T . Its effect leads to the loss of shell stability. The nature of this influence depends on the magnitude of the preheating.

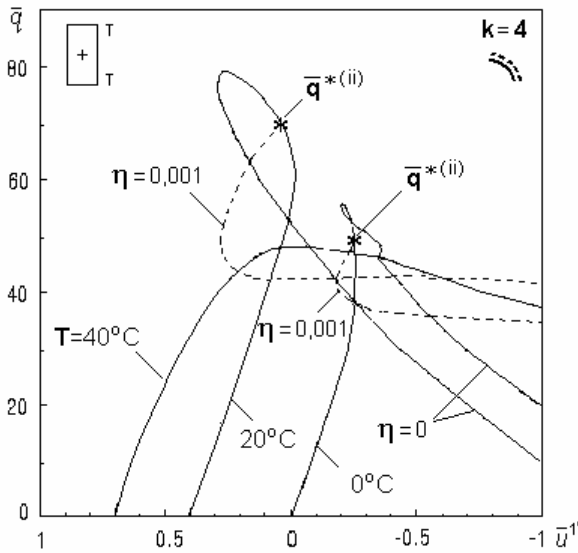


Fig. 9. The $\bar{q} - \bar{u}$ curves of the spherical panel for different levels of preheating

The evolution of the $\bar{q} - \bar{u}$ curves for the spherical panel depending on the magnitude of the preheating is shown in Fig. 9. In the absence of heating ($T = 0^\circ\text{C}$) and for a panel heated only to $T = 20^\circ\text{C}$, the $\bar{q} - \bar{u}$ curves have a rather complex shape. In the domain of the upper critical load \bar{q}_{cr}^{up} , loops appear and there are branching points ($\bar{q}^* < \bar{q}_{cr}^{up}$), detected using the Method (i) (see 4.1).

Introducing a small non-symmetric perturbation to the mid-surface of the perfect shell, according to the Method (ii) ($\eta = 0.001$), allowed refining the value of \bar{q}^* and reaching a new branch of the solution (dashed curve). In the vicinity of this point, the shell's deformation transitions from the axisymmetric form to an adjacent non-axisymmetric one. The $\bar{q} - \bar{u}$ curves corresponding to heating the

panel to $T = 40^\circ\text{C}$ are simpler in shape, reflecting the general loss of stability of the shallow shell due to central snapping.

This change in the $\bar{q} - \bar{u}$ curves is explained by the heating effect. Preheating of the panel causes it to bulge in the direction opposite to the applied pressure, increasing the rise of the panel (Fig. 10). The hotter the panel gets, the greater its rise becomes. For comparison, the initial shape of the shell is shown in the figure as a bold dash-dotted line labeled ($T = 0^\circ, q = 0$).

Buckling of a non-preheated panel ($T = 0^\circ\text{C}$) is characterized by the formation of an axisymmetric dent ($T = 0^\circ\text{C}, q_{cr}^{up}$).

Heating the shell by $T = 20^\circ\text{C}$ results in a volumetric expansion and an increase in the panel's rise by up to $0,4h$ (Fig. 10, a). The deformed shape of the panel after heating is denoted on the figure as ($T = 20^\circ\text{C}, q = 0$). Shell buckling occurs through the formation of an axisymmetric dent ($T = 20^\circ\text{C}, q_{cr}^{up}$), as in the case of the non-preheating panel ($T = 0^\circ\text{C}$). The shapes of the non-preheating ($T = 0^\circ\text{C}$) and preheating ($T = 20^\circ\text{C}$) panels at the branching point «*» (at the moment of loading \bar{q}^*) are non-axisymmetric. They have two dents ($T = 20^\circ\text{C}, q^*$).

A larger preheating of the shell by $T = 40^\circ\text{C}$ increases the panel rise by an amount $0,7h$ ($T = 40^\circ\text{C}, q = 0$; Fig. 10b). Due to the enhanced bulging effect, the $\bar{q} - \bar{u}$ curve takes the form shown

in Fig. 9, characteristic of a global stability loss by snap-through of the central portion near the pole ($T = 40^\circ\text{C}$, q_{cr}^{up} ; Fig. 10b). Branching points in the pre-critical deformation domain are not observed.

It should be noted that for panels with a clamped edge, such effects are absent. For these panels, the $\bar{q} - \bar{u}$ curves are simple, and branching points in the pre-critical deformation domain are not present.

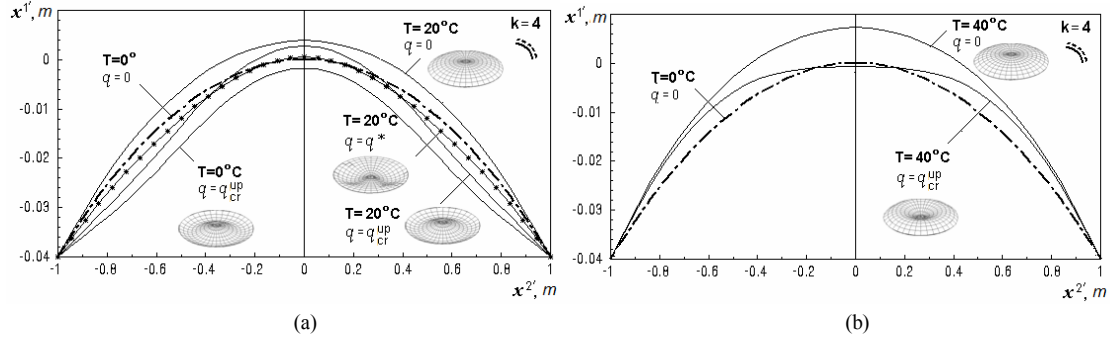


Fig. 10. Deformation and buckling shapes of the spherical panel

6.3. The effect of non-uniform thermomechanical loading on the behavior of a shell with a stepped variable thickness is shown using examples of panels with channels and ribs.

6.3.1. A shallow spherical panel of square plan with curvature parameter $K = 2a^2/(Rh) = 32$ is considered. The shell's casing, of thickness h , is weakened on the inner side by four channels of width $b_c = 2h$ and depth $h_c = 0.3h$. The longitudinal axes of the channels are located at a distance $a/3$ from the shell contour. The panel is simply supported along its contour. The input data are as follows: $h = 0.01\text{ m}$, $a = 60h$, $R = 225h$, $E = 20.59 \cdot 10^4\text{ MPa}$, $\nu = 0.3$, $\alpha = 0.12 \cdot 10^{-4}\text{ deg}^{-1}$.

First, the panel is heated: uniformly through the thickness and nonuniformly over the plan. It is then additionally loaded by a uniformly distributed pressure. Thus, as in the previous cases, the shell is subjected to two thermomechanical loading regimes, with the type of action remaining unchanged at each stage. However, at the first stage ($n = 1$), the panel heating is non-uniform in the plan (see 5.1.3). Algorithmically, the heating is implemented according to the scheme shown in Fig. 7. At the second stage ($n = 2$), a uniform pressure acts under the fixed temperature field T [15].

Four cases of non-uniform heating and uniform pressure of a shell with a stepped variable thickness are considered:

(i) pressure (for reference), denoted in the Figures as 1. q ;

(ii) preheating the shell's sections with channels by $T = 40^\circ\text{C}$ degrees followed by pressure at constant temperature (2. $T_{40^\circ}^c, q$);

(iii) preheating the shell's casing by $T = 40^\circ\text{C}$ degrees followed by pressure at constant temperature (3. $T_{40^\circ}^{sc}, q$);

(iv) preheating the entire shell followed by pressure at constant temperature (4. $T_{40^\circ}^c + T_{40^\circ}^{sc}, q$).

Naturally, the greatest effect of the combined thermomechanical loading on the value of the upper critical load \bar{q}_{cr}^{up} is exerted by the preheating of the entire shell (4th case, Fig. 11). This heating results in the greatest increase in stiffness. The value of \bar{q}_{cr}^{up} for the three heating types gradually increases by 6%, 12%, and 18%, respectively, compared with the non-preheating shell (1st case).

The developed functional approach to load specification made it possible to assess the effect of the sequence of combined thermomechanical loading on the shell with channels (see 5.2.2). The regime of this combined thermomechanical action is as follows.

At the first loading stage ($n = 1$), the panel is subjected simultaneously to pressure and uniform heating (5. $q + T_{40^\circ}^0, q$). The panel is heated by temperature $T = 40^\circ\text{C}$ until the pressure reaches the

upper critical point $\bar{q}^0 = \bar{q}_{cr}^{up0} = 178.79$ of the 1th case (1. q). From this moment onward, further variation of pressure occurs under a fixed temperature field. This corresponds to the second loading stage ($n = 2$).

A comparison has been performed to evaluate the influence of the heating sequence on shell behavior: preheating (4th case) versus simultaneous heating and pressure (5th case) (see Fig. 12).

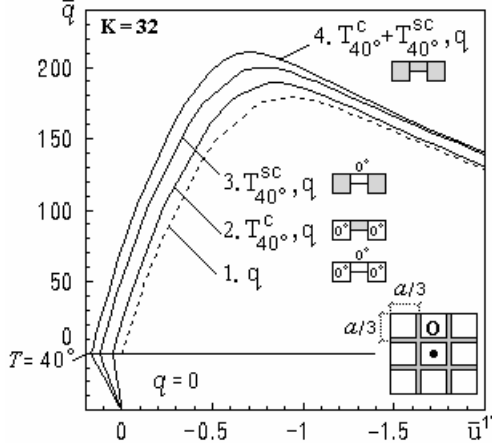


Fig. 11. Load-deflection curves of the panel center for four cases of non-uniform preheating

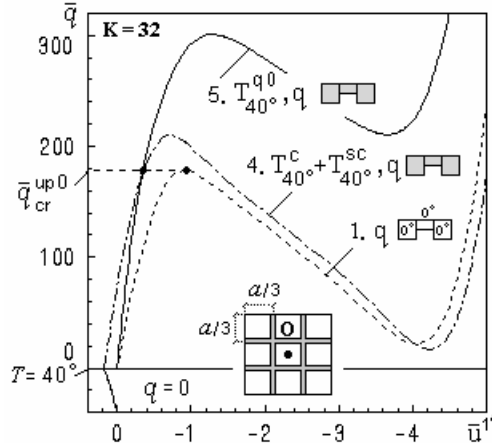


Fig. 12. Effect of sequential and simultaneous thermomechanical loading on panel stability

With preheating, the upper critical load is $\bar{q}_{cr}^{up4} = 210.36$, which is 18% higher than \bar{q}_{cr}^{up0} . With simultaneous heating and pressure, the upper critical load increases significantly to $\bar{q}_{cr}^{up5} = 300.91$, representing a 68% increase. At the same time, the lower critical load also increases substantially to $\bar{q}_{cr}^{lw5} = 210.50$, compared to $\bar{q}_{cr}^{lw0} = 22.48$ and $\bar{q}_{cr}^{lw4} = 17.22$ in the other cases.

The deformation shapes of the panel at the load level $\bar{q} = \bar{q}_{cr}^{up0}$ (Fig. 13) demonstrate qualitatively similar deformation patterns for the considered thermomechanical loading regimes. For all loading types, branching points and branch-merging points are detected only along the unstable domain of the $\bar{q} - \bar{u}$ curves (Fig. 12), that is, between the upper and lower critical loads.

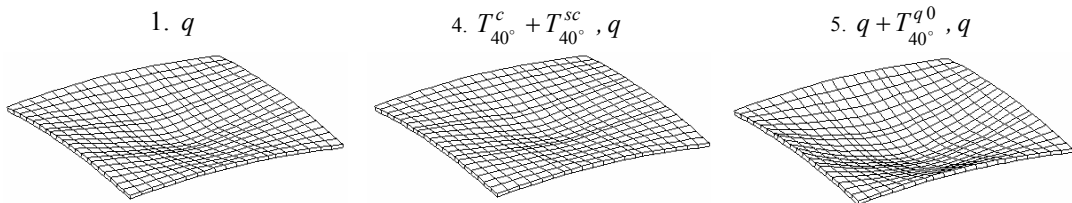


Fig. 13. Deformation shapes of the panel at the loading level $\bar{q} = \bar{q}_{cr}^{up0}$

Characteristic changes in the total deformation energy of the shell $\bar{W} = W / (Eh^3)$ and its components (membrane energy \bar{W}_m and bending energy \bar{W}_b) are shown in Figure 14. For simultaneous thermomechanical loading (5th case) the instant ($\bar{q} = \bar{q}_{cr}^{up0}$) the heating is terminated is represented by the salient kink point on the curves, and the rate of increase in strain energy decreases. This is explained by the increase in shell stiffness due to the action of the temperature field. In the precritical domain, the deformation energy increases mainly due to the membrane component, whereas in the postcritical domain, the bending component becomes dominant.

Analysis indicates that the increase in the upper critical load \bar{q}_{cr}^{up} in all heating scenarios is due to the direction of the thermal field. When heat and pressure (5th case) are applied simultaneously, the upper critical load \bar{q}_{cr}^{up} increases by 43.0% compared with the 4th case where they act sequentially. In this case, the lower critical load \bar{q}_{cr}^{hw} increases significantly by a factor of 12. These effects are due to the increased stiffness of the heated shell.

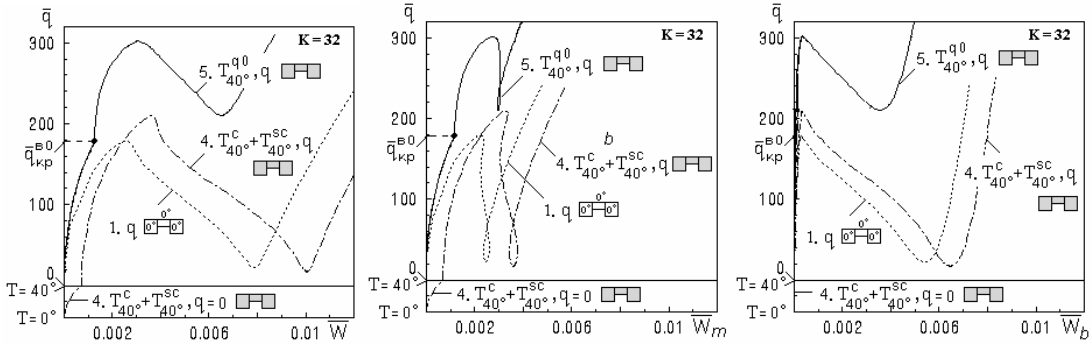
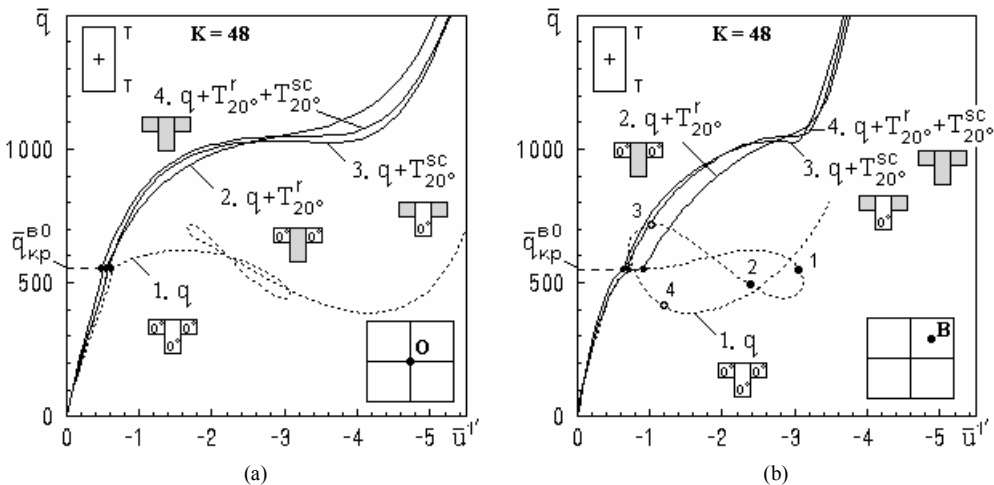


Fig. 14. Load–deformation energy curves

6.3.2. The nonlinear deformation and buckling of a ribbed panel, characterized by the curvature parameter $K = 48$ ($a = 60h$, $R = 150h$), is considered. The shell is reinforced from the inside with two cross ribs (height $h_r = 3h$, width $b_r = 2h$, length $a = 60h$). The ribs and the shell are made of the same material.

A combined regime of thermomechanical loading on the shell (see 5.2.2) is studied, consisting of two stages. In the first stage, the shell is subjected simultaneously to a non-uniform heating and a uniform pressure ($n = 1$). The structural elements are heated by temperature $T = 20^\circ\text{C}$ (see 5.1.3) following the scheme shown in Fig. 6. The simultaneous thermomechanical loading continues until the pressure reaches $\bar{q} = \bar{q}^0$. Afterwards, with the temperature field held constant, only the pressure acts ($n = 2$). The type of loading on each stage remains unchanged. All three heating scenarios are applied until the dimensionless parameter of the first upper critical load reaches $\bar{q}^0 = \bar{q}_{cr}^{up0} = 553.22$. This value has been for the shell under the action of pressure (1. q).

The load–deflection $\bar{q} - \bar{u}$ curves at points O and B (Fig. 15) indicate that, upon loss of stability, the shell undergoes similar significant changes for all loading cases. All heating scenarios of the shell elements result in a substantial increase in the stiffness of the ribbed panel.



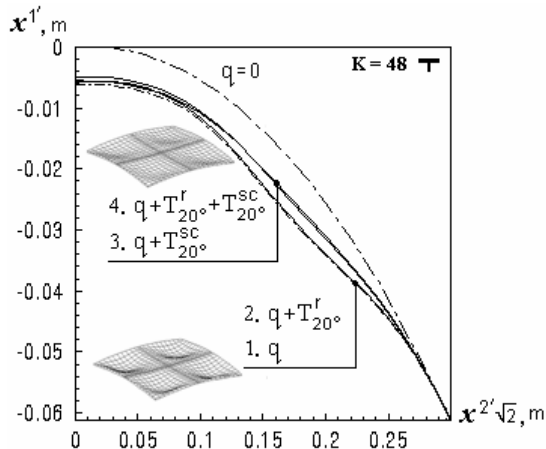


Fig. 16. Deformation shapes of the ribbed panel at $\bar{q}^0 = \bar{q}_{cr}^{up0}$

stiffness. The behavior of the ribbed panel is similar for all heating regimes. The deformation shapes are identical, and the $\bar{q} - \bar{u}$ curves in the post-critical domain practically coincide.

Conclusions

An integral approach is applied to the analysis of geometrically nonlinear deformation, buckling, post-buckling behavior, and natural vibrations of thin inhomogeneous shells under static thermomechanical loading. A comprehensive investigation of the stability and natural vibrations of shells subjected to static thermomechanical loading is implemented by means of a stepwise algorithm. A distinctive feature of the proposed method and the algorithm developed on its basis is the ability to accurately analyze both the pre-buckling and post-buckling states of shell deformation with various thickness features, including ribs, channels, and similar structural elements.

The specificity of the method and algorithm lies in the adopted methodology for prescribing thermomechanical loading as a function. This enables the definition of various loading regimes and the description of complex combined thermomechanical effects on the structure that may be close to real operating conditions. In addition, the developed method provides the capability, in the analysis of nonlinear deformation and buckling of shells to determine solution branching points and to trace adjacent equilibrium branches in the pre-buckling domain.

The features of the method and algorithm are demonstrated through a series of specially selected benchmark problems.

REFERENCES

1. Bathe K.-J., Wilson E.L. Numerical methods in finite element analysis. – Prentice-Hall Inc., Englewood Cliffs, N.J., 1976. – 528 p.
2. Zenkevich O. Metod konechnykh elementov v tekhnike (Finite element method in engineering). – M.: Mir. – 1975. – 541 p. (in Russian).
3. Oden J. Konechnyye elementy v nelineynoy mekhanike sploshnykh sred (Finite Elements in Nonlinear Continuum Mechanics). – M.: Mir, 1976. – 464 p. (in Russian).
4. Rikards R.B. Metod konechnykh elementov v teorii obolochek i plastin (Finite element method in the theory of shells and plates). – Riga: Zinatne, 1988. – 284 p. (in Russian).
5. Sakharov A.S., Kislokiy V.N., Kirichevsky V.V. et al. Metod konechnykh elementov v mekhanike tverdykh tel (Finite element method in solid mechanics). – K.: Vishcha school. Glavnoye izdatel'stvo, 1982. – 480 p. (in Russian).
6. Chapelle D., Bathe K.J. The finite element analysis of shells – Fundamentals. Series: Computational fluid and solid mechanics. – Berlin; Heidelberg: Springer, 2011. – 410 p.
7. Reddy J.N. Theory and Analysis of Elastic Plates and Shells, Second Edition. – CRC Press, 2006. – 568 p.
8. Lukianchenko O., Kostina O. The finite element method in problems of the thin shells theory. – LAP LAMBERT, Academic Publishing, Beau Bassin, Mauritius, 2019 – 134 p.
9. Bazhenov, V.A., Luk'yanchenko, O.O., Vorona, Y.V., Vabyshevych, M.O. The influence of shape imperfections on the stability of thin spherical shells // Strength of Materials, 2021. – 53(6). – P. 842-851. <https://doi.org/10.1007/s11223-022-00351-0>
10. Solodei I.I., Vabyshevich M.O., Stryhun R.L. Semianalytical finite elements method efficiency in the geometrically nonlinear elastic-plastic problems // Strength of Materials and Theory of Structures: Scientific-and-technical collected articles. – Kyiv: KNUBA, 2019. – Issue 103. – P. 71- 81. DOI: 10.32347/2410-2547.2019.103.71-81

Fig. 15. The $\bar{q} - \bar{u}$ curves of the spherical ribbed panel for four cases of combined pressure and heating action

The deformation shapes of the shell at the load level $\bar{q}^0 = \bar{q}_{cr}^{up0}$ are practically identical, with the maximum deflection located at the centers of the panel quarters (Fig. 16). Such a deformation pattern is characteristic specifically of non-shallow panels. In the figure, the mid-surface deformation curves are shown along the diagonal. The initial shape is indicated by a dash-dotted line labeled as $q = 0$.

As in the previous cases, the increase in the critical load \bar{q}_{kp}^6 for all heating cases is associated with the effect of the temperature field, which leads to an increase in shell

11. Bazhenov V.A., Maksym'yuk Y.V., Martyniuk I.Yu., Maksym'yuk O.V. Napivanalitichnyy metod skinchennykh elementiv v prostorovykh zadakhakh deformuvannya, ruynuvannya ta formozminennya til skladnoyi struktury (Semi-analytical finite element method in spatial problems of deformation, destruction and shape change of bodies of complex structure). – Kyiv: Vydavnytstvo «Karavella», 2021. – 280 p. (in Ukrainian).
12. Solodei I.I., Kozub Yu.G., Stryhun R.L., Shovkivska V.V. Analiz alhorytmiv rozv'yazannya heometrychno nelineynykh zadakh mekhaniky v skhemi napivanalitichnoho metodu skinchennykh elementiv (Algorithms analysis for solving geometrically nonlinear mechanics problems in the scheme of the semi-analytical finite element method) // Strength of Materials and Theory of Structures: Scientific-and-technical collected articles- K.: KNUBA, 2022. – Issue 109. - P. 109-119. DOI: 10.32347/2410-2547.2022.109.109-119 (in Ukrainian).
13. Bazhenov V.A., Solovei N.A. Nonlinear deformation and buckling of elastic inhomogeneous shells under thermomechanical loads // Int Appl Mech., 2009. –45 (9). – P. 923–953.
14. Bazhenov V.A., Krivenko O.P., Solovei M.O. Nelineine deformuvannya ta stiikist pruzhnykh obolonok neodnorodnoi struktury (Nonlinear deformation and stability of elastic shells with inhomogeneous structure). – K.: ZAT «Vipob», 2010. – 316 p. ISBN: 978-966-646-097-7 (in Ukrainian)
15. Krivenko O.P., Lizunov P.P., Kalashnikov O.B. Momentna skhema skinchennykh elementiv u zadakhakh termostiikosti i vlasnykh kolyvan' pruzhnykh neodnorodnykh obolonok: Monohrafiya (Moment scheme of finite elements in problems of thermal stability and natural oscillations of elastic inhomogeneous shells: Monograph). – Kyiv: Vydavnytstvo «Karavella», 2024. – 179 p. ISBN 978-966-969-168-2 (in Ukrainian).
16. Kryvenko, O.P., Lizunov, P.P., Vorona, Y.V., Kalashnikov, O.B. Modeling of nonlinear deformation, buckling, and vibration processes of elastic shells in inhomogeneous structure // Int Appl Mech, 2024. – 60 (3). 464- 478. <https://doi.org/10.1007/s10778-024-01298-2>.
17. Krivenko O.P., Lizunov P.P. Investigation of nonlinear deformation, buckling and natural vibrations of elastic shells under thermomechanical loads using a universal three-dimensional finite element // Strength of Materials and Theory of Structures: Scientific-and-technical collected articles. – Kyiv: KNUBA, 2025. – Issue 114. – P. 35-43. DOI: 10.32347/2410-2547.2025.114.35-43
18. Blokh V.I. Teoriya uprugosti (Theory of elasticity). – Kharkov: Kharkiv State University, 1964. – 483 p. (in Russian)
19. Novatsky V. Teoriya uprugosti (Theory of elasticity). – M.: Mir, 1975. –872 p. (in Russian)
20. Rabotnov Yu.N. Mekhanika tverdogo deformiruyemogo tela (Mechanics of a solid deformable body). – M.: Nauka, 1988. – 712 p. (in Russian).
21. Vol'mir A.S. Ustoychivost' deformiruyemykh sistem (Stability of deformable systems). – M.: Nauka, 1967. – 984 p. (in Russian).
22. Teoriya vetvleniya i nelineynyye zadachi na sobstvennyye znacheniya (Branching theory and nonlinear eigenvalue problems) / Ed. J. B. Keller, S. Antman. – M.: Mir, 1974. – 254 p. (in Russian).
23. Kantor B.Ya. Nelineynyye zadachi teorii neodnorodnykh plogykh obolochek (Nonlinear problems in the theory of inhomogeneous shallow shells). – Kyiv: Naukova dumka, 1974. – 136 p. (in Russian)
24. Bushnell D. Analysis of ring-stiffened shells of revolution under combined thermal and mechanical loading // AIAA Journal, 1971 –9(3). – P. 401–410 <https://doi.org/10.2514/3.6194>
25. Bushnell D., Smith S. Stress and buckling of nonuniformly heated cylindrical and conical shells // AIAA Journal, 1971. 9 (12). – P. 2314–2321 <https://doi.org/10.2514/3.6515>
26. Zamula G.N., Ierusalimsky K.M., Karpova G.S. Issledovaniye ustoychivosti i termoustoychivosti slozhnykh podkreplennykh konstruksiy (Study of stability and thermal stability of complex reinforced structures) // Uch. Zapiski TsAGI. – 1989. – Vol. XX. – N4. – P. 84-87 (in Russian).
27. Valishvili N.V. Metody rascheta obolochek vrashcheniya na ETSVM (Methods for calculating shells of revolution on a digital computer). – M.: Mashinostroenie, 1976. – 278 p. (in Russian).
28. Hubertus J. Weinitschke. The effect of asymmetric deformations on the buckling of shallow spherical shells // Journal of the Aerospace Sciences, 1962. – Vol. 29 (9). - P. 1141-1142 <https://doi.org/10.2514/8.9733>.
29. Poterya ustoychivosti i vupuchivaniye konstruksiy: teoriya i praktika / Pod red. Dzh. Tompsona i Dzh. Khanta (Loss of stability and buckling of structures: theory and practice / Ed. J. Thompson and J. Hunt). – M.: Nauka, 1991. – 424 p. (in Russian).

Стаття надійшла 16.03.2026

Кривенко О.П., Лізунов П.П., Калашніков О.Б.

ОСОБЛИВОСТІ СКІНЧЕННОЕЛЕМЕНТНОГО МОДЕЛЮВАННЯ АНАЛІЗУ СТІЙКОСТІ ПРУЖНИХ ОБОЛОНОК НЕОДНОРОДНОЇ СТРУКТУРИ ПРИ ТЕРМОМЕХАНІЧНИХ ВПЛИВАХ

Метод дослідження поведінки пружних неоднорідних оболонок базується на геометрично нелінійних співвідношеннях тривимірної теорії термопружності, положеннях моментної схеми скінчених елементів і використанні універсального просторового скінченного елемента, що модифікується за рахунок додаткових змінних параметрів. Для аналізу геометрично нелінійного деформування, втрати стійкості, закритичної поведінки та власних коливань оболонок при дії статичних термомеханічних навантажень застосовується інтегральний підхід. Комплексне дослідження стійкості та власних коливань оболонок, що знаходяться під дією статичних термомеханічних навантажень, реалізується кроковим алгоритмом. Відмінною рисою методу та побудованого на його основі алгоритму є можливість точно аналізувати як докритичний, так і закритичний стан деформування оболонок з різними особливостями за товщиною, в тому числі з ребрами, каналами тощо. Специфікою методу та алгоритму є прийнята методологія задавання термомеханічного навантаження як складної функції. Це надає змогу задавати як різні режими навантаження, так і описувати складні комбіновані термомеханічні впливи на конструкцію, які можуть бути близькими до реальних. Окрім того, розроблений метод наділений можливістю при розрахунках нелінійного деформування та втрати стійкості оболонок визначати точки розгалуження розв'язків та отримувати вихід на суміжні гілки розв'язку у закритичній області деформування. Особливості методу та алгоритму продемонстровані на низці спеціально підібраних задач.

Ключові слова: тонка неоднорідна оболонка, геометрично нелінійне деформування, стійкість, термомеханічне навантаження, універсальний тривимірний скінченний елемент, моментна схема скінчених елементів.

Krivenko O.P., Lizunov P.P., Kalashnikov O.B.

FEATURES OF FINITE ELEMENT MODELING FOR BUCKLING ANALYSIS OF ELASTIC SHELLS WITH INHOMOGENEOUS STRUCTURE UNDER THERMOMECHANICAL LOADS

The method for studying the behavior of elastic inhomogeneous shells is based on geometrically nonlinear relationships of the three-dimensional theory of thermoelasticity, the principles of the finite element moment scheme, and the use of a modifiable universal 3d finite element with additional variable parameters. For the analysis of geometrically nonlinear deformation, buckling, post-buckling behavior, and natural vibrations of shells under static thermomechanical loading, an integral approach is employed. A comprehensive study of the stability and natural vibrations of shells subjected to static thermomechanical loading is implemented using a stepwise algorithm. A distinctive feature of the method and the algorithm developed on its basis is the capability to accurately analyze both the pre-buckling and post-buckling states of shell deformation with various thickness features, including ribs, channels, etc. The specificity of the method and algorithm lies in the adopted methodology for prescribing thermomechanical loading as a function. This enables the definition of various loading regimes and the description of complex combined thermomechanical effects on the structure that may be close to real operating conditions. In addition, the developed method provides the capability, in the analysis of nonlinear deformation and buckling of shells to determine solution branching points and to trace adjacent equilibrium branches in the pre-buckling domain. The features of the method and algorithm are demonstrated through a series of specially selected benchmark problems.

Key words: thin inhomogeneous shell, geometrically nonlinear deformation, buckling, thermomechanical loading, universal 3D finite element, finite element moment scheme.

УДК 539.3

Кривенко О.П., Лізунов П.П., Калашніков О.Б. Особливості скінченноелементного моделювання аналізу стійкості пружних оболонок неоднорідної структури при термомеханічних навантаженнях // Опір матеріалів і теорія споруд: наук.-тех. збірн. – Київ: КНУБА, 2026. – Вип. 116. – С. 50-66.

Розглянуті деякі практичні питання комп'ютерного моделювання та аналізу процесів геометрично нелінійного деформування тонких оболонок ступінчасто-змінної товщини при дії статичних термомеханічних навантажень. Методологія дослідження оболонок систем з різними конструктивними елементами за товщиною спирається на використання універсального просторового скінченного елемента, що модифікується за рахунок додаткових змінних параметрів.

Іл. 16. Бібліогр. 29 назв.

UDC 539.3

Krivenko O.P., Lizunov P.P., Kalashnikov O.B. Features of Finite Element Modeling for Buckling Analysis of Elastic Shells with Inhomogeneous Structure under Thermomechanical Loads // Strength of Materials and Theory of Structures: Scientific-and-technical collected articles. – Kyiv: KNUBA, 2026. – Issue 116. – P. 50-66.

This article examines some practical aspects of computer modeling and analysis of geometrically nonlinear deformation processes in thin shells with stepwise variable thicknesses under static thermomechanical loads. The methodology for studying shell systems with structural elements of varying thickness is based on the use of a modifiable universal 3D finite element with additional variable parameters.

Fig. 16. Ref. 29.

Автор (науковий ступінь, вчене звання, посада): кандидат технічних наук, старший науковий співробітник, провідний науковий співробітник НДІ будівельної механіки Київського національного університету будівництва і архітектури, КРИВЕНКО Ольга Петрівна

Адреса робоча: 03037, Україна, м. Київ, проспект Повітряних Сил, 31, КНУБА, НДІ будівельної механіки

Робочий тел.: +38(044) 245-48-29

E-mail: olakop@ukr.net

ORCID ID: <https://orcid.org/0000-0002-1623-9679>

Автор (науковий ступінь, вчене звання, посада): доктор технічних наук, професор, завідувач кафедри будівельної механіки Київського національного університету будівництва і архітектури ЛІЗУНОВ Петро Петрович

Адреса робоча: 03037, Україна, м. Київ, проспект Повітряних Сил, 31, КНУБА, кафедра будівельної механіки

E-mail: lizunov@knuba.edu.ua

ORCID ID: <https://orcid.org/0000-0003-2924-3025>

Автор (науковий ступінь, вчене звання, посада): кандидат технічних наук, старший науковий співробітник Державного науково-технічного центру ядерної та радіаційної безпеки, КАЛАШНИКОВ Олександр Борисович

Адреса робоча: 03142, Україна, м. Київ, вул. Василя Стуса, 35-37, Державний науково-технічний центр ядерної та радіаційної безпеки

E-mail: kalash2d@gmail.com

ORCID ID: <https://orcid.org/0009-0009-7825-9809>